environmental sciences proceedings

MDPI

Proceeding Paper

Jakarta's 2020 New Year Flood Assessment by Rainfall-Runoff-Inundation (RRI) Model †

Yeremia Immanuel Sihombing [1], Akbar Rizaldi [1], Mohammad Farid [1], N. Fajar Januriyadi [2] and Idham Riyando Moe [3,*]

[1] Center for Coastal and Marine Development, Institute for Research and Community Services, Institut Teknologi Bandung, Jalan Ganesha No.10, Kota Bandung 40132, Indonesia; yeremia.sihombing97@gmail.com (Y.I.S.); akbar@ftsl.itb.ac.id (A.R.); mfarid@ftsl.itb.ac.id (M.F.)
[2] Department of Civil Engineering, Pertamina University, Jalan Teuku Nyak Arief, RT.7/RW.8, Simprug, Kec. Kby. Lama, Kota Jakarta Selatan 12220, Indonesia; nurul.fj@universitaspertamina.ac.id
[3] Directorate General of Water Resources, Ministry of Public Works and Housing, Jalan Pattimura No. 20, Kebayoran Baru, Jakarta Selatan 12110, Indonesia.
* Correspondence: idham.moe@gmail.com
† Presented at the 7th International Electronic Conference on Water Sciences, 15–30 March 2023; Available online: https://ecws-7.sciforum.net.

Abstract: Floods hit Jakarta and several areas in Ciliwung-Cisadane Watershed. The rain that occurred on 31 December 2019 stopped briefly and continued until 1 January 2020. As a result, several areas were flooded for several days. It is said that the rain that occurred was the largest in history. At least the rainfall station at Halim Perdanakusuma Airport recorded a rainfall with an intensity of 377 mm/day. That makes a question about how much discharge was generated by the rainfall. This study was conducted to assess the flood discharge and the inundated area caused by the rain in 2020 New Year's Eve. The Rainfall-Runoff-Inundation (RRI) is utilized to simulate the flood discharge and inundation using the 1D-2D hydraulic-hydrology model. This model also calculates infiltration and subsurface flow with the Green-Ampt equation. Besides, the rainfall data uses rain data recorded by the ground station and the topography uses SRTM data from the United States Geological Survey (USGS). Then, the flood discharge obtained from the model is compared with the flood return period. The return periods of the flood that are compared are 2, 5, 10, 25, 50, and 100 years. The result shows that the flood that occurred on 1 January 2020 is bigger than the flood with a return period of 100 years. This means that the rainfall has the biggest effect to the flood rather than other factors.

Keywords: Flood, Jakarta, 2020, RRI

Citation: Sihombing, Y.I.; Rizaldi, A.; Farid, M.; Januriyadi, N.F.; Moe, I.R. Jakarta's 2020 New Year Flood Assessment by Rainfall-Runoff-Inundation (RRI) Model. *Environ. Sci. Proc.* **2023**, *4*, x. https://doi.org/10.3390/xxxxx

Academic Editor(s):

Published: 15 March 2023

1. Introduction

Flood is a natural process of a body of water which rises to overflow land that not normally submerged due to high flow of runoff or sea surge water [1–3]. There are several types of floods including fluvial flood, pluvial flood, and coastal flood [4–6]. Pluvial flood could be caused by rain process, which produce amount of water flow on the surface called runoff. The runoff simply determined by rainfall, the area of catchment, and the respond catchment which represented by runoff coefficient [7]. Many factors can be caused flood, included meteorological, geomorphology, and anthropogenic [8–15]. The meandering river shape conditions, especially if the riverbed narrow through, the water with a large discharge can derive an overflow [16]. Some places that previously did not experience floods have become areas affected by flooding due to changes in land use in the upstream area [17,18]. In urban areas, flooding occurs due to illegal settlement and sedimentation which reduce the capacity of a river or channel [19–21]. In cold climate regions, early spring snowmelt combined with heavy rainfalls can also cause flooding

[22]. Seawater levels rising and high rainfall which are the effects of climate change are also the cause of flooding in some areas [23–26]. Social behavior that occurs in the community indirectly can also have an impact on runoff, for example, urbanization. Urbanization will affect the land use of some area, which changes in land cover that will affect the runoff [27,28].

Jakarta was hit by flooding again in early 2020, January 1st. 103 locations were submerged by the flood around the province of DKI Jakarta and West Java which located in Ciliwung–Cisadane Watershed [29]. Flooding occurred due to high rainfall intensity on 31 December 2019, exactly 1 day before. At least 2 stations from 8 stations around the DKI Jakarta area recorded rainfall of more than 300 mm, this is the highest rainfall for the last 25 years [30].

Flooding in the Ciliwung–Cisadane watershed is not a new issue. It has happened since the 1660s [31]. An increase in discharge in the Ciliwung river was allegedly triggered by a change in the land-use change in the upstream area to become a tea plantation [33]. Some countermeasures to deal with increased runoff in the Ciliwung River have been carried out since 1970's and some have been implemented to date [33]. However, over time some areas began to develop, the problem of flooding in the Ciliwung–Cisadane Watershed was increasingly complex and flooding still occurred.

The floods that have not yet been solved have caused several areas in the Ciliwung Cisadane watershed to still suffer from flooding. It caused material and non-material losses. This loss is not only caused by the size of the affected area but also due to the unpreparedness of an area in the face of a disaster. The more prepared an area is in dealing with disasters, it will reduce the losses suffered [34]. This preparedness is not only related to the protection of an area against a flood but all the effort of an area in dealing with the flood disaster itself. This preparedness includes structural and non-structural efforts [35]. The integration and sustainability of preparation, protection and ability to respond effectively are the key to the resilience to flood disaster [36].

Many studies about the flood in Ciliwung–Cisadane Watershed have been done with different considerations. Climate change, land subsidence, land use change, even social phenomenon such as urbanization have been considered in several studies about flooding in Ciliwung–Cisadane Watershed [37,38]. The future projection of flood in Ciliwung basin has been discussed in several studies as well. Moe et al. have conducted a study related to the possibility of flooding in Jakarta with scenarios caused by land subsidence and combined with land-use changes [39,40]. Emam et al. show how the climate change and land-use change influence the flood behavior in Jakarta, it increases the peak flow of a 50-year return period in 2030 by 130% [41]. Januriyadi et al. not only did study about the future flood but also analyze the flood risk due to climate change and urban development in 2050 and show that the risk is multiplied extremely [42].

Although there are many studies have been conducted about flooding in the Ciliwung–Cisadane watershed, due to the occurrence floods almost every year makes the flood is still interesting to be investigated. To predict future changes is very interesting but projecting current events to past predictions is not a bad idea indeed. The news related to Jakarta floods in the early 2020s startled Indonesia, moreover the information that the rain that occurred was the biggest in history. The question is how big the flood discharge is due to that rain event. To be more specific, which return period is equivalent to the coming flood on 1 January 2020. Today, it is not impossible to assess the flood after it happened. In 2018, Moe et al have been conducted a rapid assessment to predict the affected area due to the flood in Upper Citarum River Basin [43]. The aim of this study is to know the characteristic of flood in 2020 new year eve by using rapid assessment.

2. Materials and Methods

2.1. Study Area

The study is located at Ciliwung–Cisadane Watershed, as shown in Figure 1. It consists of 15 river basins which accumulatively has area 5269.84 km^2. It administratively covers 3 Provinces, 9 cities/municipalities as follow Province of DKI Jakarta (5 cities), Bogor, Depok, Bekasi, and Tangerang. the study area is located between latitude 5°59′28″ S to latitude 6°47′18″ S and longitude 106°24′45″ E to longitude 107°12′54″ E.

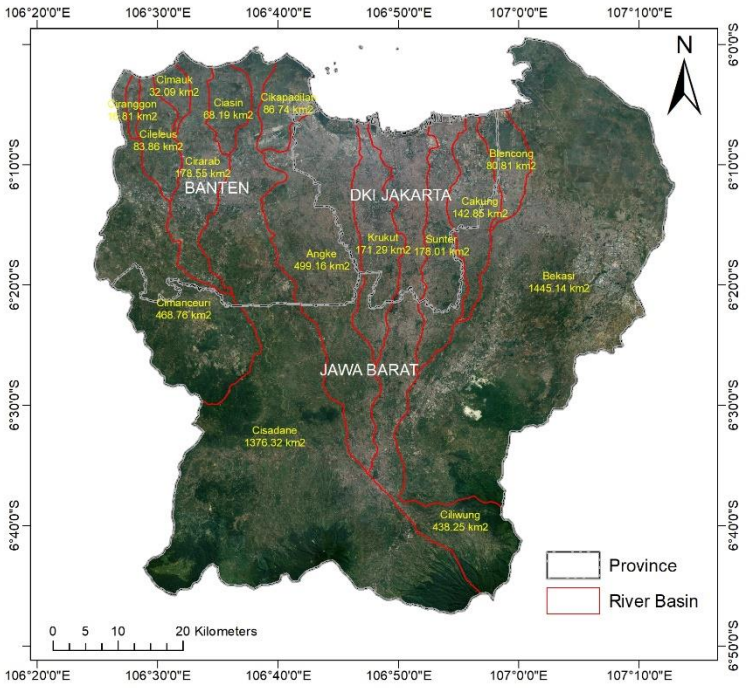

Figure 1. Study Area.

2.2. Data

2.2.1. Precipitation Data

The precipitation data were collected from 24 rainfall stations in Ciliwung–Cisadane Watershed during the flood event. All of the rain stations are located around the study area as shown in Figure 2a,b presents the rainfall distribution throughout the river area using Inverse Distance Weighted Interpolation (IDW) method. The IDW method is the most frequently used deterministic method and can be applied for the data whose distribution was characterised by a very big range [43]. From the data, the maximum rainfall during this event reached 376 mm. This condition is higher than the predicted rainfall 100 years return period in Halim Station which is 340 mm [45].

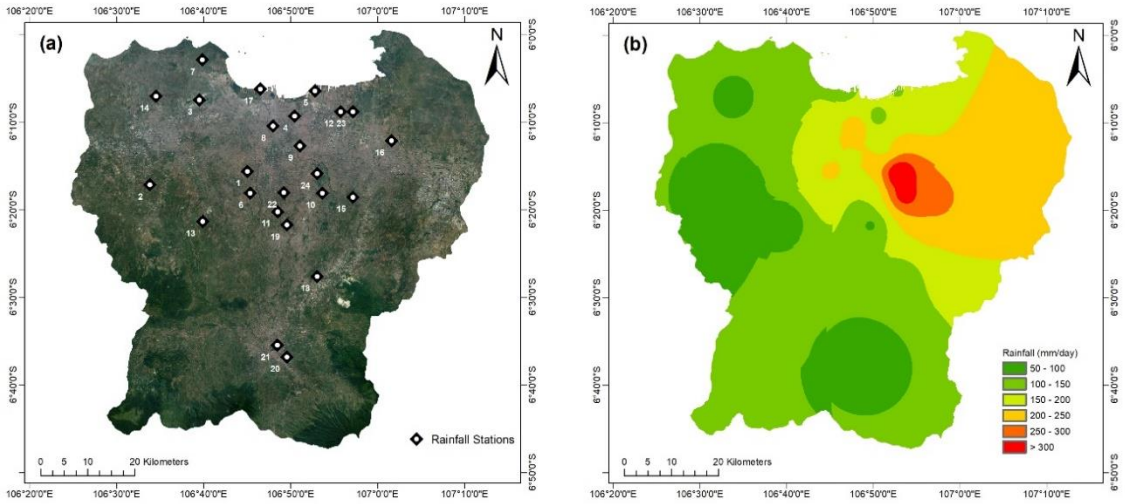

(**a**) (**b**)

Figure 2. Rainfall datasets in the study area: (**a**) Rainfall station locations; (**b**) Rainfall distribution on 1 January 2020.

Table 1. List of rainfall stations.

No	Rainfall Station	No	Rainfall Station
1	Stasiun Klimatologi Tanggerang Selatan	13	AWS Puspitek
2	Stasiun Meteorologi Curug	14	ARG Sepatan
3	Stasiun Meteorologi Cengkareng	15	ARG Jatiasih
4	Stasiun Meteorologi Kemayoran	16	ARG Teluk Pucung
5	Stasiun Maritim Tanjung Priok	17	ARG Muara
6	Pos Hujan Bd Ciputat	18	ARG Jagorawi
7	Pos Hujan Teluk Naga	19	AWS UI
8	ARG Tomang	20	ARG Katulampa
9	ARG Manggarai	21	AWS IPB
10	AWW TMII	22	Pos Hujan Ragunan
11	ARG Ciganjur	23	Pos Hujan Rorotan
12	ARG Sukapura	24	TNI AU Halim

The predicted return period rainfall will be utilized as input in calibrated model to see the characteristic of various return periods of flood. The return period of rainfall calculation was developed by Januriyadi et al. [42]. The forecasting is used BMKG (Meteorological and Geophysical Institution of Indonesia) rainfall dataset in a period of 1986–2010 as a reference. The data were distributed throughout study area as presented in Figure 3. Compared with the rainfall that occurs on 1 January, maximum rainfall on that event exceeded the maximum data in 100-years period which has good corresponding with the previous study.

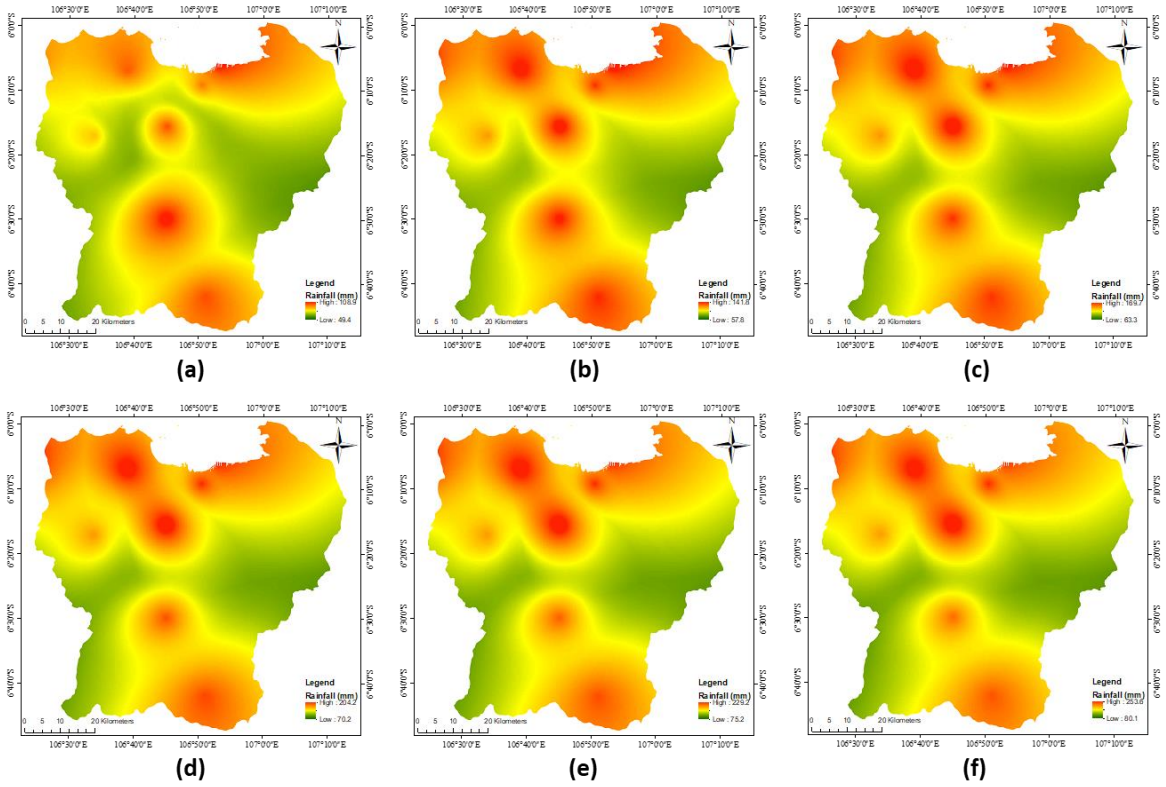

Figure 3. Rainfall return period datasets (**a**) Rainfall return period of 2 years, (**b**) Rainfall return period of 5 years, (**c**) Rainfall return period of 10 years, (**d**) Rainfall return period of 25 years, (**e**) Rainfall return period of 50 years and (**f**) Rainfall return period of 100 years.

2.2.2. Topography

The topography data is derived from the Digital Elevation Model (DEM) obtained from the Shuttle Radar Topography Mission (SRTM). The data was open-source data provided by the United States Geological Survey (USGS). For the SRTM, the vertical accuracy is 16 m for 90% confidence level [46].

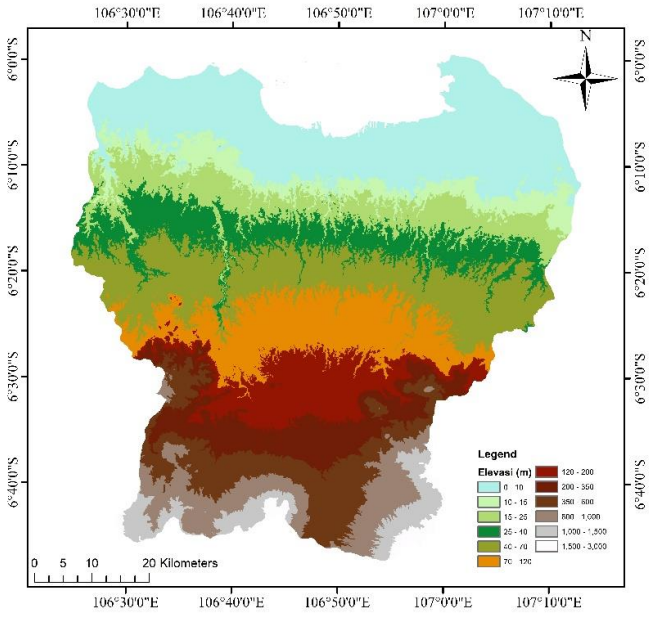

Figure 4. Digital Elevation Model (DEM) of Ciliwung-Cisadane Watershed.

Figure 4 presents the topographical condition of Ciliwung–Cisadane Watershed. The resolution of DEM that used in this calculation was based on 1 arc second or about 30 m. Nevertheless, the resolution has been scaled up to 100 m due to computational issues. The numbers of row and column of the pixels are 885 and 891. The upscaling of DEM resolution increases the Topography Index (TI) of DEM because of the nesting process of several grids with different TI into one grid with one TI [47]. The consequences are the area or grid that should be submerged to become dry area and vice versa.

2.2.3. Land Cover

Land over was obtained from Global Land Cover Characterization Version 2 (GLCC-V2). This database has been developed by The U.S. Geological Survey (USGS), the University of Nebraska-Lincoln (UNL), and the European Commission's Joint Research Centre (JRC) since 1992. The land cover projection has 1-km nominal spatial resolution and unique geographic elements. The land classification for this model has been simplified from GLCC-V2 for calculation purpose (Figure 5).

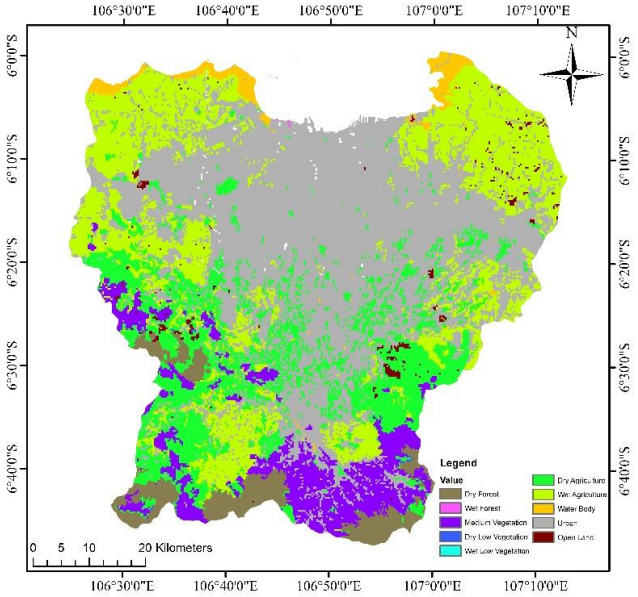

Figure 5. Land cover of Ciliwung–Cisadane Watershed.

Each of land cover classification has different characteristics in the model based on soil conditions as presented in Table 2. In this model, the river was distinguished from the water bodies. The river location was auto generated by RRI model from Digital Elevation Model.

Table 2. The characteristic of land cover.

Parameters	Land Cover		
	Clay	Loam	Sandy Clay Loam
Soil depth (m)	1	1	1
Porosity (-)	0.475	0.463	0.398
k_v (m/s)	0–8.33×10^{-8}	0–9.44×10^{-7}	0–4.17×10^{-7}
S_f	0.361	0.089	0.219
k_a (m/s)	0–0.3	0–0.3	0–0.3
Unsat. porosity (-)	0	0	0
Beta	8	8	8

2.3. Rainfal-Runoff-Inundation (RRI) Model

Rainfall-runoff-inundation (RRI) model is a two-dimensional model with the simplified equation. This model is capable to simulates rainfall-runoff and flood inundation at the same time, it is also designed to be used immediately after the disaster and it can be useful as the tool to analyze large-scale flood as well [48]. Figure 6 shows how the river and slope treated separately. Besides, it assumes that the river channel location is in the same grid cells as the slope. A river channel is considered as a centerline in a grid cell. It indicates an extra flow path between grid cells and the actual river course. On the other hand, the slope cells function as the two-dimensional simulation area of the lateral flow. Hence, there are two water depths for slope grid cells in water channels, i.e. the channel and the slope (floodplain) itself.

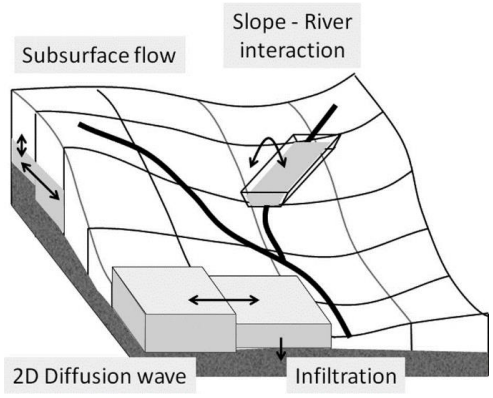

Figure 6. Rainfall-runoff-inundation (RRI) model schematic diagram (Source: Sayama et al., 2012).

The inflow-outflow interaction between the river and slope is based on different overflowing formulae. The calculation depends on water-level and levee-height conditions. This model generated based on mass balance Equation (1) for governing equation of flow rate equation. The momentum equation is derived from the governing equation of the model in x directions Equation (2) and y directions Equation (3).

$$\frac{\partial h}{\partial t} + \frac{\partial q_x}{\partial x} + \frac{\partial q_y}{\partial y} = r - f \quad (1)$$

$$\frac{\partial q_x}{\partial t} + \frac{\partial u q_x}{\partial x} + \frac{\partial v q_x}{\partial y} = -g\,h\,\frac{\partial H}{\partial x} - \frac{\tau_x}{\rho_w} \quad (2)$$

$$\frac{\partial q_y}{\partial t} + \frac{\partial u q_y}{\partial x} + \frac{\partial v q_y}{\partial y} = -g\,h\,\frac{\partial H}{\partial y} - \frac{\tau_y}{\rho_w} \quad (3)$$

where h is the height of water from the local surface, q_x and q_y are the unit width discharges in x and y directions, u and v are the flow velocities in x and y directions, r is the rainfall intensity, H is the height of water from the datum, ϱw is the density of water, g is the gravitational acceleration, τ_x and τ_y the shear stresses in x and y directions.

The RRI model separates the calculation of discharge and hydraulic gradient relationship. Hence, the simulation of surface and subsurface flow proceeds in the same algorithm. Besides, the kinematic rainfall-runoff wave and diffusive wave approximation are also derived in this model. The kinematic wave is calculated with the assumption that water surface slope as the hydraulic gradient. On the other hand, diffusion stream approximation is utilized to form the streamflow equation.

The calibration process is done by doing a flood simulation of flood events on 1 January. Then the inundation area from the simulation is compared with the inundation map obtained from remote sensing by satellite at the same time. The model is well-calibrated if the result shows similarities to the inundation obtained from remote sensing.

3. Result and Discussion

3.1 Model Calibration

The model was calibrated before being used to simulate the return period flood. It was calibrated with a flood event that occurred on 1 January 2020. The simulation has calculated the distribution of flood inundation in the condition of maximum water depth and compared by the inundated area from satellite data at the same event (Figure 7). Figure 7 shows the comparison of simulated flood inundation and flood inundation of sentinel 1A acquired on 2 January 2020. The flood inundation of sentinel 1A generated using an algorithm that proposed by Chini et al [48]. The algorithm can detect the flood water not only on bare soil but also on the urban regions. Even though the Sentinel 1-A acquired a day after flood event, some inundation still remains on the land. Figure 7 shows a similar inundation on the north-east part between simulation and satellite data. Whereas in the middle part near ocean, the figure shows that the simulated inundation areas are larger than the satellite data. Because the flood waters in urban area of Jakarta receded on 2 January 2020.

The inundation in this model consists of local inundation and large-scale inundation. The local inundation is defined as local water depth that is barely moving. Accordingly, this type of inundation has a limited range of area and shallow water depth. On the other hand, the large-scale inundation is water depth that is growing around the river with a wide range of areas.

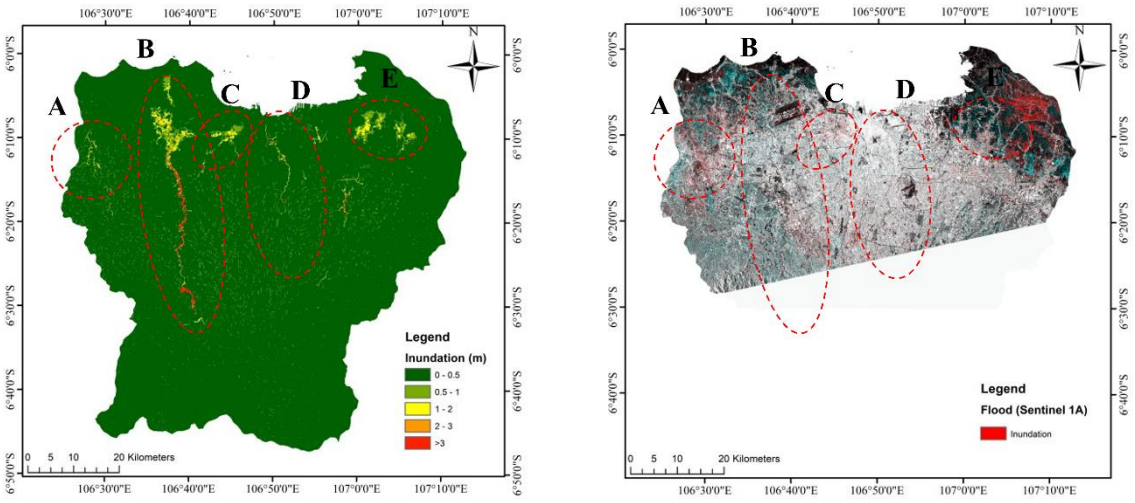

(**a**) (**b**)

Figure 7. Rapid Assessment of Jakarta Flood Inundation: (**a**) simulated 1 January flood inundation (**b**) flood inundation of sentinel 1A acquired on 2 January 2020.

Circle A, B, C, D and E present large-scale inundation during the simulation period. The locations of the circles are in Cimanceuri, Cisadnae, Angke, Ciliwung, and Bekasi River Basins respectively. Table 3 shows the approximation of the total affected area due to river inundation. The total area of river inundation is approximately 106.54 km^2. Hence, the percentage of river inundation area during this event is 56.51% towards the total inundation area.

Table 3. Large Scale Inundation Area.

Location	River Basin	Inundation Area (km^2)	Affected City(ies)
A	Cimanceuri	6.3	Tanggerang
B	Cisadane	51.05	Tanggerang,
C	Angke	11.9	West Jakarta

D	Ciliwung	5.03	East Jakarta, South Jakarta, Central Jakarta
E	Bekasi	32.26	Bekasi

3.2. Model Application

The model that has calibrated is used to do the return period analysis of the flood. The flood return periods are simulated in mostly the same condition with the main simulation. Nevertheless, the precipitation is used as an input in these simulations was modified to rainfall return periods that has forecasted by from historical rainfall data. The period of rainfall that used in this calculation is 2 years, 5 years, 10 years, 25 years, 50 years, and 100 years. The results of these simulations were shown in Figure 8. Most of the large-scale inundation in each return period located in the same locations i.e., Cimanceuri, Cisadnae, Angke, Ciliwung, and Bekasi River Basins. Therefore, the location of large-scale inundation is the same as the main simulation.

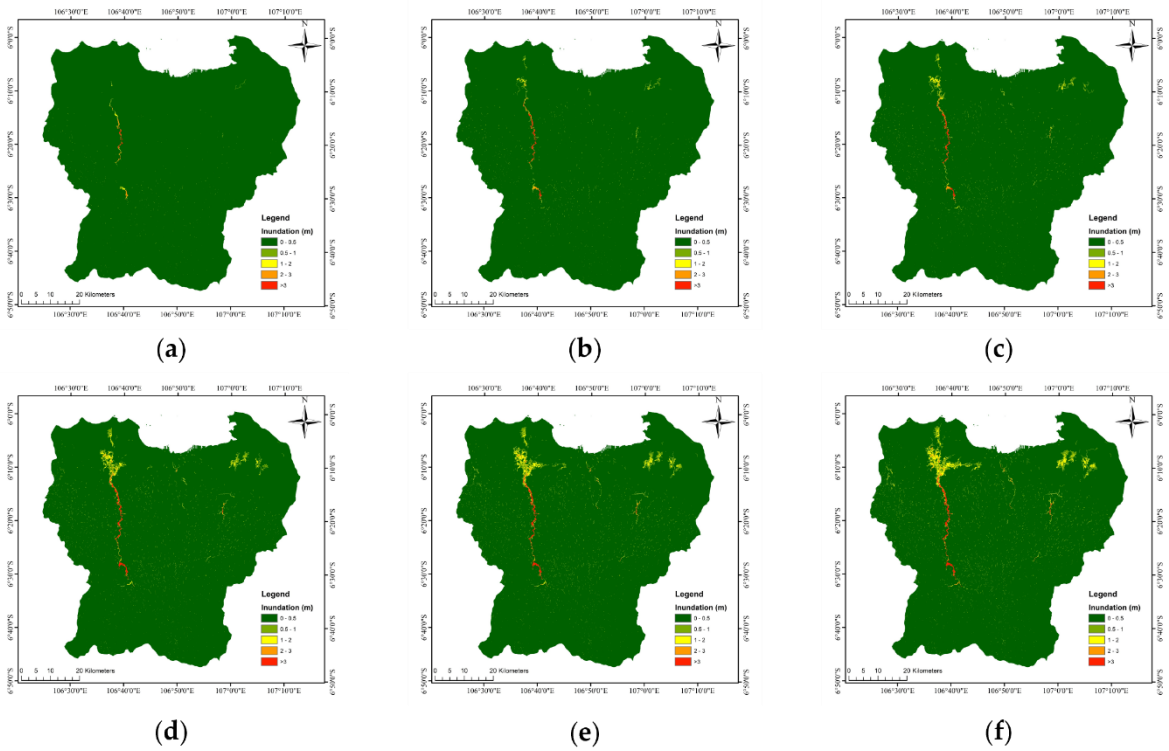

Figure 8. The inundation of flood returns period (a) Flood return period of 2 years, (b) Flood return period of 5 years, (c) Flood return period of 10 years, (d) Flood return period of 25 years, (e) Flood return period of 50 years and (f) Flood return period of 100 years.

Table 4. The characteristic of flood returns period.

Flood Simulation	Volume (1000 m³)	Max. Discharge (m³/s)
Return period of 2 years	16475	199.75
Return period of 5 years	22059	260.88
Return period of 10 years	25797	297.85
Return period of 25 years	30397	340.95
Return period of 50 years	33450	365.67
Return period of 100 years	36355	389.97
Jakarta Flood	40204	420.76

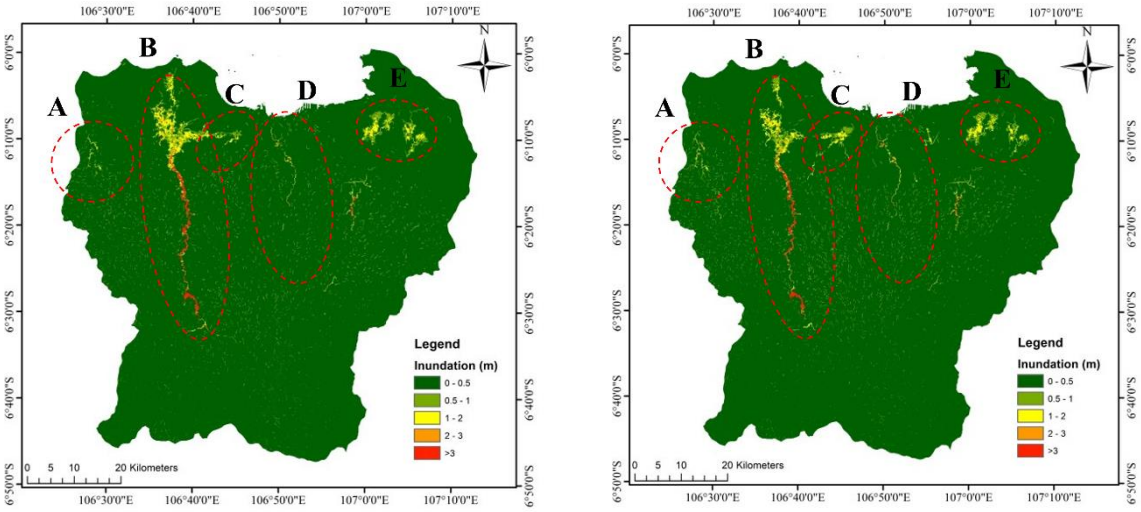

(**a**) (**b**)

Figure 9. The comparison between: (**a**) 100 yearly flood and (**b**) Flood on 1 January 2020.

The area and volume of the inundation are calculated in the return period flood simulation. Then the area and volume of inundations are compared with the inundation characteristic of the flood that occurred on 1 January 2020. The Table 4 shows that the closest area of return period floods to the flood on 1 January is the flooding with 100 yearly floods. The inundated area of both flood maps shows quite similar (Figure 9). It strengthens the evidence that the floods that occurred on 1 January were floods with a return period of 100 years. Whereas the rainfall on that day is greater than the rainfall with a return period of 100 years. The flood may not as big as the rainfall due to the spatial distribution of rainfall. The variability of rainfall spatial distribution could affected the amount of flood discharge which generates different flood [50,51].

The flood discharge was calculated on the main model and flood return period. It measured with RRI hydro calculation on Water Gate Manggarai in Ciliwung River '06°12'27.48" S and 106°50'54.55" E). The maximum discharge of each model was presented in Table 4**.** The discharge of the main model was compared with flood 2, 5, 10, 25, 50 and 100 years return periods (Figure 10). The maximum discharge of main model exceeded 100-years return period. Therefore, the main model has better corresponding with raingauge data which is bigger than 100 years return period rain data.

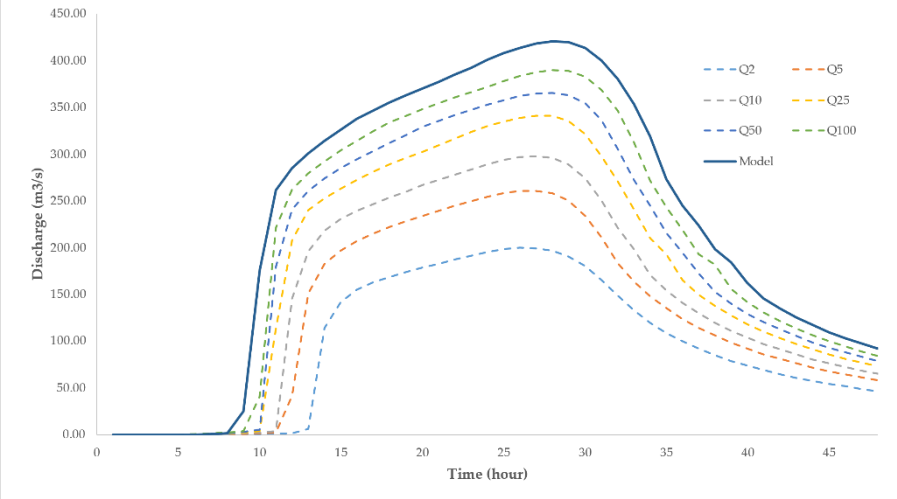

Figure 10. Discharge on Water Gate Manggarai.

4. Conclusions

This study attempts to do a rapid assessment of flood on 1 January 2020, in Jakarta and several areas of the Ciliwung–Cisadane Watershed. The study was conducted to find out the return period of the flood that occurred. Rainfall-Runoff-Inundation (RRI) is a distributed model that is able to simulate rainfall-runoff and flooding simultaneously. The model based on the inundation map from remote sensing satellite was calibrated with ground station rainfall. The resolution of Digital Elevation Model (DEM) that too high hindered the simulation process, it made the resolution of DEM should be decreased. The DEM is upscaled, then the grid size is changed from 30 m to 100 m. After the model has been calibrated, a return period flood model is performed with a return period rainfall input. There are six return periods of rainfall are being simulated, there are 2, 5, 10, 25, 50, and 100 years of the return period of rainfall.

The discharge and inundation area of all return periods is compared with the simulation of flood on 1 January. The comparison showed that the discharge extent on 1 January is exceeded the discharge with a return period of 100 years. This result corresponds with the rain recorded at several rainfall stations which surpassed the 100-year rainfall return period. Thus, there are several conclusions. First, the flood that occurred on 1 January 2020, is superior than a 100-year return period of flood. Second, the rainfall, which is the biggest in the history, is the main effect of the flood of this flood because it exceeded the 100-year return period of rainfall.

In this study, the DEM implemented in this model has low resolution because the limitation of data sources. In addition, the model need to be compared with the existing discharge during the flood. This conditions need to be considered in future research.

References

1. Chow, V.T.; Maidment, D.R.; Mays, L.W. Applied Hydrology (Letters); 1988.
2. Penning-Rowsell, E.C.; Ward, R. Floods: A Geographical Perspective. *Geogr. J.* **1980**, *146*, 139, https://doi.org/10.2307/634110.
3. Webster, T.L.; Forbes, D.L.; Dickie, S.; Shreenan, R. Using topographic lidar to map flood risk from storm-surge events for Charlottetown, Prince Edward Island, Canada. *Can. J. Remote. Sens.* **2004**, *30*, 64–76, https://doi.org/10.5589/m03-053.
4. Merz, B.; Hall, A.J.; Disse, M.; Schumann, A.H. Fluvial flood risk management in a changing world. *Nat. Hazards Earth Syst. Sci.* **2010**, *10*, 509–527, https://doi.org/10.5194/nhess-10-509-2010.
5. Zhou, Q.; Mikkelsen, P.S.; Halsnæs, K.; Arnbjerg-Nielsen, K. Framework for economic pluvial flood risk assessment considering climate change effects and adaptation benefits. *J. Hydrol.* **2012**, *414-415*, 539–549, https://doi.org/10.1016/j.jhydrol.2011.11.031.
6. Ganguli, P.; Merz, B. Extreme Coastal Water Levels Exacerbate Fluvial Flood Hazards in Northwestern Europe. *Sci. Rep.* **2019**, *9*, 13165, https://doi.org/10.1038/s41598-019-49822-6.
7. Ferreira, S.; Ghimire, R. Forest cover, socioeconomics, and reported flood frequency in developing countries. *Water Resour. Res.* **2012**, *48*, W08529, https://doi.org/10.1029/2011wr011701.
8. Li, F.; Wang, L.; Zhao, Y. Evolvement rules of basin flood risk under low-carbon mode. Part I: Response of soil organic carbon to land use change and its influence on land use planning in the Haihe basin. *Environ. Monit. Assess.* **2017**, *189*, 377, https://doi.org/10.1007/s10661-017-6101-5.
9. Maes, J.; Molombe, J.M.; Mertens, K.; Parra, C.; Poesen, J.; Che, V.B.; Kervyn, M. Socio-political drivers and consequences of landslide and flood risk zonation: A case study of Limbe city, Cameroon. *Environ. Plan. C Politi- Space* **2019**, *37*, 707–731, https://doi.org/10.1177/2399654418790767.
10. Mahmoud, S.H.; Gan, T.Y. Urbanization and climate change implications in flood risk management: Developing an efficient decision support system for flood susceptibility mapping. *Sci. Total. Environ.* **2018**, *636*, 152–167, https://doi.org/10.1016/j.scitotenv.2018.04.282.
11. Blume, T.; Zehe, E.; Bronstert, A. Rainfall—Runoff response, event-based runoff coefficients and hydrograph separation. *Hydrol. Sci. J.* **2007**, *52*, 843–862, https://doi.org/10.1623/hysj.52.5.843.
12. Baker, V.R.; Pickup, G. Flood geomorphology of the Katherine Gorge, Northern Territory, Australia. *Geol. Soc. Am. Bull.* **1987**, *98*, 635, https://doi.org/10.1130/0016-7606(1987)98<635:fgotkg>2.0.co;2.
13. Bauer, B.O.; Baker, V.R.; Kochel, R.C.; Patton, P.C. Flood Geomorphology. *Geogr. Rev.* **1990**, *80*, 341, https://doi.org/10.2307/215322.
14. Texier, P. Floods in Jakarta: When the extreme reveals daily structural constraints and mismanagement. *Disaster Prev. Manag.* **2008**, *17*, 358–372, https://doi.org/10.1108/09653560810887284.
15. Lee, M.-H.; Bae, D.-H. Climate Change Impact Assessment on Green and Blue Water over Asian Monsoon Region. *Water Resour. Manag.* **2015**, *29*, 2407–2427, https://doi.org/10.1007/s11269-015-0949-3.
16. Baker, V.R. Stream-Channel Response to Floods, with Examples from Central Texas. *Geol. Soc. Am. Bull.* **1977**, 88, 1057–1071. https://doi.org/10.1130/0016-7606(1977)88<1057:SRTFWE>2.0.CO;2.
17. Dasanto, B.D.; Pramudya, B.; Boer, R.; Suharnoto, Y. Effects of Forest Cover Change on Flood Characteristics in the Upper Citarum Watershed. *J. Manaj. Hutan Trop. (J. Trop. For. Manag.)* **2014**, *20*, 141–149, https://doi.org/10.7226/jtfm.20.3.141.
18. Farid, M.; Mano, A.; Udo, K. Modeling flood runoff response to land cover change with rainfall spatial distribution in urbanized catchment. *J. Jpn. Soc. Civ. Eng. Ser. B1 (Hydraulic Eng.)* **2011**, *67*, I_19–I_24, https://doi.org/10.2208/jscejhe.67.i_19.
19. Rosso, R.; Rulli, M.C. An integrated simulation method for flash-flood risk assessment: 2. Effects of changes in land-use under a historical perspective. *Hydrol. Earth Syst. Sci.* **2002**, *6*, 285–294, https://doi.org/10.5194/hess-6-285-2002.
20. Lane, S.N.; Reid, S.C.; Tayefi, V.; Yu, D.; Hardy, R.J. Reconceptualising coarse sediment delivery problems in rivers as catchment-scale and diffuse. *Geomorphology* **2008**, *98*, 227–249, https://doi.org/10.1016/j.geomorph.2006.12.028.
21. Rizaldi, A.; Moe, I.R.; Farid, M.; Aribawa, T.M.; Bayuadji, G.; Sugiharto, T. Study of flood characteristic in Cikalumpang River by using 2D flood model. *MATEC Web Conf.* **2019**, *270*, 04010, https://doi.org/10.1051/matecconf/201927004010.
22. Zaghloul, M.S.; Ghaderpour, E.; Dastour, H.; Farjad, B.; Gupta, A.; Eum, H.; Achari, G.; Hassan, Q.K. Long Term Trend Analysis of River Flow and Climate in Northern Canada. *Hydrology* **2022**, *9*, 197, https://doi.org/10.3390/hydrology9110197.
23. Karim, M.F.; Mimura, N. Impacts of climate change and sea-level rise on cyclonic storm surge floods in Bangladesh. *Glob. Environ. Chang.* **2008**, *18*, 490–500, https://doi.org/10.1016/j.gloenvcha.2008.05.002.
24. Hallegatte, S.; Ranger, N.; Mestre, O.; Dumas, P.; Corfee-Morlot, J.; Herweijer, C.; Wood, R.M. Assessing climate change impacts, sea level rise and storm surge risk in port cities: A case study on Copenhagen. *Clim. Change* **2010**, *104*, 113–137, https://doi.org/10.1007/s10584-010-9978-3.
25. Darsan, J.; Asmath, H.; Jehu, A. Flood-risk mapping for storm surge and tsunami at Cocos Bay (Manzanilla), Trinidad. *J. Coast. Conserv.* **2013**, *17*, 679–689, https://doi.org/10.1007/s11852-013-0276-x.
26. Buchanan, M.K.; Kopp, R.E.; Oppenheimer, M.; Tebaldi, C. Allowances for evolving coastal flood risk under uncertain local sea-level rise. *Clim. Change* **2016**, *137*, 347–362, https://doi.org/10.1007/s10584-016-1664-7.
27. Du, J.; Qian, L.; Rui, H.; Zuo, T.; Zheng, D.; Xu, Y.; Xu, C.-Y. Assessing the effects of urbanization on annual runoff and flood events using an integrated hydrological modeling system for Qinhuai River basin, China. *J. Hydrol.* **2012**, *464-465*, 127–139, https://doi.org/10.1016/j.jhydrol.2012.06.057.

28. Aich, V.; Liersch, S.; Vetter, T.; Fournet, S.; Andersson, J.C.; Calmanti, S.; van Weert, F.H.; Hattermann, F.F.; Paton, E.N. Flood projections within the Niger River Basin under future land use and climate change. *Sci. Total. Environ.* **2016**, *562*, 666–677, https://doi.org/10.1016/j.scitotenv.2016.04.021.
29. BNPB Editorial. Hujan Ekstrem Penyebab Banjir Jakarta. Available online: https://bnpb.go.id/berita/hujan-ekstrem-penyebab-banjir-jakarta (accessed on 16 May 2020).
30. Biro Komunikasi Publik Kementrian PUPR. Menteri Basuki Siapkan Langkah Penanganan Banjir di Jakarta dan Sekitarnya. Available online: https://pu.go.id/berita/view/17794/menteri-basuki-siapkan-langkah-penanganan-banjir-di-jakarta-dan-sekitarnya (accessed on 16 May 2020).
31. Caljouw, M.; Nas, P.J.; Pratiwo, M. Flooding in Jakarta: Towards a blue city with improved water management. *J. Humanit. Soc. Sci. Southeast Asia* **2009**, *161*, 454–484, https://doi.org/10.1163/22134379-90003704.
32. Kurniawan, B.E.; Corps, M. Adapting cities to climate variability and change: Balance between community engagement and supporting facilitation roles of the local government to reduce the impact of climate change. In Proceedings of the Human(e) Settlements: The Urban Challenge Conference, Johannesburg, South Africa, 17–21 September 2012; p. 194.
33. Octavianti, T.; Charles, K. The evolution of Jakarta's flood policy over the past 400 years: The lock-in of infrastructural solutions. *Environ. Plan. C Politi- Space* **2019**, *37*, 1102–1125, https://doi.org/10.1177/2399654418813578.
34. Miceli, R.; Sotgiu, I.; Settanni, M. Disaster preparedness and perception of flood risk: A study in an alpine valley in Italy. *J. Environ. Psychol.* **2008**, *28*, 164–173, https://doi.org/10.1016/j.jenvp.2007.10.006.
35. Petry, B. Keynote Lecture: Coping with Floods: Complementarity of Structural and Non-Structural Measures. In *Flood Defence*; Science Press: New York, NY, USA, 2002; pp. 60–70.
36. Hadihardaja, I. K.; Kuntoro, A. A.; Farid, M. Flood Resilience for Risk Management: Case Study of River Basin in Indonesia. *Glob. Asp.* **2013**, *3*, 16–19.
37. Budiyono, Y.; Aerts, J.C.J.H.; Tollenaar, D.; Ward, P.J. River flood risk in Jakarta under scenarios of future change. *Nat. Hazards Earth Syst. Sci.* **2016**, *16*, 757–774, https://doi.org/10.5194/nhess-16-757-2016.
38. Mishra, B.K.; Emam, A.R.; Masago, Y.; Kumar, P.; Regmi, R.K.; Fukushi, K. Assessment of future flood inundations under climate and land use change scenarios in the Ciliwung River Basin, Jakarta. *J. Flood Risk Manag.* **2017**, *11*, S1105–S1115, https://doi.org/10.1111/jfr3.12311.
39. Moe, I.R.; Kure, S.; Januriyadi, N.F.; Farid, M.; Udo, K.; Kazama, S.; Koshimura, S. Effect of land subsidence on flood inundation in Jakarta, Indonesia. *J. Jpn. Soc. Civ. Eng. Ser. G (Environmental Res.* **2016**, *72*, I_283–I_289, https://doi.org/10.2208/jscejer.72.i_283.
40. Moe, I.R.; Kure, S.; Januriyadi, N.F.; Farid, M.; Udo, K.; Kazama, S.; Koshimura, S. Future projection of flood inundation considering land-use changes and land subsidence in Jakarta, Indonesia. *Hydrol. Res. Lett.* **2017**, *11*, 99–105, https://doi.org/10.3178/hrl.11.99.
41. Emam, A.R.; Mishra, B.K.; Kumar, P.; Masago, Y.; Fukushi, K. Impact Assessment of Climate and Land-Use Changes on Flooding Behavior in the Upper Ciliwung River, Jakarta, Indonesia. *Water* **2016**, *8*, 559, https://doi.org/10.3390/w8120559.
42. Januriyadi, N.F.; Kazama, S.; Moe, I.R.; Kure, S. Evaluation of future flood risk in Asian megacities: A case study of Jakarta. *Hydrol. Res. Lett.* **2018**, *12*, 14–22, https://doi.org/10.3178/hrl.12.14.
43. Moe, I.R.; Rizaldi, A.; Farid, M.; Moerwanto, A.S.; Kuntoro, A.A. The use of rapid assessment for flood hazard map development in upper citarum river basin. *MATEC Web Conf.* **2018**, *229*, 04011, https://doi.org/10.1051/matecconf/201822904011.
44. Bronowicka-Mielniczuk, U.; Mielniczuk, J.; Obroślak, R.; Przystupa, W. A Comparison of Some Interpolation Techniques for Determining Spatial Distribution of Nitrogen Compounds in Groundwater. *Int. J. Environ. Res.* **2019**, *13*, 679–687, https://doi.org/10.1007/s41742-019-00208-6.
45. Liu, J.; Doan, C.D.; Liong, S.-Y.; Sanders, R.; Dao, A.T.; Fewtrell, T. Regional frequency analysis of extreme rainfall events in Jakarta. *Nat. Hazards* **2015**, *75*, 1075–1104, https://doi.org/10.1007/s11069-014-1363-5.
46. Jarvis, A.; Rubiano, J.; Nelson, A.; Farrow, A.; Mulligan, M. *Practical Use of SRTM Data in the Tropics—Comparisons with Digital Elevation Models Generated from Cartographic Data*; Centro Internacional de Agricultura Tropical (CIAT): Cali, Colombia, 2004.
47. Zhang, H.; Li, Z.; Saifullah, M.; Li, Q.; Li, X. Impact of DEM Resolution and Spatial Scale: Analysis of Influence Factors and Parameters on Physically Based Distributed Model. *Adv. Meteorol.* **2016**, *2016*, 8582041, https://doi.org/10.1155/2016/8582041.
48. Sayama, T.; Ozawa, G.; Kawakami, T.; Nabesaka, S.; Fukami, K. Rainfall–runoff–inundation analysis of the 2010 Pakistan flood in the Kabul River basin. *Hydrol. Sci. J.* **2012**, *57*, 298–312, https://doi.org/10.1080/02626667.2011.644245.
49. Chini, M.; Pelich, R.; Pulvirenti, L.; Pierdicca, N.; Hostache, R.; Matgen, P. Sentinel-1 InSAR Coherence to Detect Floodwater in Urban Areas: Houston and Hurricane Harvey as a Test Case. *Remote. Sens.* **2019**, *11*, 107, https://doi.org/10.3390/rs11020107.
50. Ogden, F.L.; Sharif, H.O.; Senarath, S.U.S.; Smith, J.A.; Baeck, M.L.; Richardson, J.R. Hydrologic analysis of the Fort Collins, Colorado, flash flood of 1997. *J. Hydrol.* **2000**, *228*, 82–100, https://doi.org/10.1016/s0022-1694(00)00146-3.
51. Arnaud, P.; Bouvier, C.; Cisneros, L.; Dominguez, R. Influence of rainfall spatial variability on flood prediction. *J. Hydrol.* **2002**, *260*, 216–230, https://doi.org/10.1016/s0022-1694(01)00611-4.